Peer-reviewed version available at Polymers 2019, 11, 765; doi:10.3390/polym11050765

Article

Synthesis of Thermo-Responsive Block-Graft Copolymer Based on PCL and PEG Analogues, and Preparation of Hydrogel *via* Click Chemistry

Pei Shang, Jie Wu, Xiaoyu Shi, Zhidan Wang, Fei Song and Shouxin Liu*

Key Laboratory of Applied Surface and Colloid Chemistry, Ministry of Education, School of Chemistry and Chemical Engineering, Shaanxi Normal University, Xi'an, 710119, P. R. China; sp13772442791@163.com (P.S.); 18375847342@163.com (J.W.); 18647847370@163.com (X.S.); 18189608643@163.com (Z.W.); 17563713257@163.com (F.S.)

* Correspondence: liushx@snnu.edu.cn; Tel.: +86-29-81530781

Abstract: The cross-linkable PCL-PEG analogues block-graft copolymer was designed and synthesized, which with the copolymer of the MEO_2MA and OEGMA as graft chains to improve the *m*PEG-*b*-PCL-*b*-*m*PEG copolymer the aqueous solution properties. And successfully prepared two hydrogels via a copper-catalyzed 1, 3-dipolar azide-alkyne cycloaddition reaction of alkyne-terminated poly[glycidyl methacrylate-*co*-2-(2-methoxyethoxy) ethyl methacrylate-*co*-oligo (ethylene glycol) methacrylate] [P(GMA-*co*-MEO_2MA-*co*-OEGMA)] with azide end-functionalized PCL-PEG analogues block-graft copolymer, and tetrakis (2-propynyloxymethyl) -methane (TPOM) and with azide end-functionalized PCL-PEG analogues block-graft copolymer. The copolymer's chemical structure was characterized by proton nuclear magnetic resonance spectroscopy and fourier transform infrared spectroscopy. The molecular weights of the copolymers were decided with gel permeation chromatography. The water solubility and temperature sensitivity of the copolymers were studied by taking digital photos and transmittance change measured by UV spectrophotometer at different temperatures. Fluorescence probes, surface tension, dynamic light scattering and transmission electron microscopy were used to analyze the micelles that copolymers self-assembly in aqueous solution. The sol-gel behavior of copolymer solutions at high concentrations was explored by vial inversion experiments. Finally, the network structure of the gels was observed by scanning electron microscopy. These conclusions indicate that these hydrogels are expected to be used as a new material in the field of biomedicine.

Keywords: ε-Caprolactone; block-graft copolymer; click chemistry; hydrogel

PACS: J0101

1. Introduction

The use of chemical techniques to synthesize biomimetic materials such as biological tissues and carriers has become one of the hotspots of research [1,2]. Hydrogel with three-dimensional network structure stands out among many chemical synthetic materials because of their good biodegradability, low immunogenicity, and the micro-environment that can truly simulate human tissues and cells on a three-dimensional scale [3-5]. Environmentally responsive hydrogels are a class of hydrogels that produce corresponding reversible changes depending on small changes in their environment, such as temperature, pH, and ion concentration [6,7]. This special property makes environmentally responsive hydrogels suitable for many sub-area of biomedical applications, such as controlling drug release, tissue engineering, gene delivery, artificial muscle, etc [8-12]. But, the

amount of the copolymer in a lot of hydrogels is limited，and the content of the rigid monomer in the comonomer directly affects swellability and mechanical properties of the hydrogels[13]. Therefore, it is necessary to designe a new type of hydrogel.

There are many ways to synthesize hydrogel, such as free radical polymerization, microemulsion polymerization, "click chemistry" [14] and the like. Among them, the monomer conversion rate of the radical polymerization method is slightly lower, and the formed macromolecular structure is not easy to control [15]. Microemulsion polymerization has a limited range of applications [16]. Click chemistry is one of the most common methods for synthesizing gels because of its ability to rapidly synthesize various compounds and at a low cost [17-19]. In particular, the monovalent copper ion in "click chemistry" catalyzes the dipolar cycloaddition reaction of azido-alkynyl group, the crosslinking reaction condition is mild, the gelation rate is controllable, and the Cu(I) in the catalyst is no toxic to cells, which determines this way is an ideal method for preparing three-dimensional network hydrogels [20,21].

It is well known that polyethylene glycol (PEG) and poly (ε-caprolactone) (PCL) are widely used in the field of biomedicine because they have the superior properties of being non-toxic, non-immune and degradable to human body [22-28]. The initial strength of PCL is high, the degradation rate is slow, and the mechanical properties are maintained for a long time. It can be applied to bone repair or tissue engineering as a material to increase toughness. However, the disadvantage of PCL in water solubility limits the application of PCL-PEG copolymer [29,30]. A PEG analogues copolymer formed by the polymerization of 2-(2-methoxy ethoxy) ethyl methacrylate (MEO_2MA) and oligoethylene glycol methyl methacrylate (OEGMA), except that having good water solubility similar to PEG, it also has unique temperature sensitivity, moreover, the molar ratio of MEO_2MA and OEGMA added to the reaction directly affects the low critical solution temperature (LCST) of the copolymer after the reaction [31-33]. Based on the above conditions, this work designed to synthesize a novel cross-linkable PCL-PEG analog block-graft copolymer, which having MEO_2MA and OEGMA monomer to improve the water solubility and temperature sensitivity properties of the PCL block.

In addition, two different crosslinkers were synthesized in this work: alkyne-terminated P(GMA-*co*-MEO_2MA-*co*-OEGMA) contain 2-(2-methoxy ethoxy) ethyl methacrylate (MEO_2MA) and oligoethylene glycol methyl methacrylate (OEGMA), given the polymer the same good water solubility and temperature sensitivity as the PCL-PEG analog block-graft copolymer. TPOM [34] can provide multiple click sites. Two hydrogels with different internal three-dimensional network densities are formed. The two hydrogels will exert their great potential value in the field of biomedicine.

2. Experimental Section

2.1. Materials

ε-Caprolactone (99%), monomethoxy poly(ethylene glycol) (M_W = 750 g·mol^{-1}), Cuprous chloride was purchased from Alfa Aesar. Stannous octoate ($Sn(Oct)_2$, 96%), Glycidyl methacrylate (99%), Pentaerythritol (98%), Tetrabutylammonium bromide were purchased from J&k. Hexamethylene diisocyanate (HMDI), 2-(2-methoxy ethoxy) ethyl methacrylate (MEO_2MA) were purchased from TCL. Propargyl bromide and *N*-dodecyl mercaptan, *N*, *N*, *N*', *N*', *N*''-pentamethyl diethylenetriamine (PMDETA) were purchased from Macleans. Sodium azide purchased from Zhengzhou Penny Chemical Reagent Factory, 2,2'-bipyridine was purchased from Guangdong Guanghua Technology Co., Ltd. Dichloromethane, n-hexane, anhydrous diethyl ether, toluene, methanol, *N*, *N*-dimethylformamide (DMF), 1,4-dioxane, acetone and other reagents were purchased from Sinopharm Chemical Reagent Co., Ltd. Among them, ε-Caprolactone should be dried with CaH_2 for 48 hours at room temperature before use. Methylene chloride was refluxed for 4 hours under the condition of adding CaH_2, and then distilled out for use. Toluene needs to be refluxed for 4 hours with the addition of an appropriate amount of Na, and distilled for use.

2.2. Synthesis

2.2.1. Synthesis of block copolymer mPEG-b-PCL-b-mPEG

Block copolymer *m*PEG-*b*-PCL-*b*-*m*PEG is synthesized by ring-opening polymerization (ROP). The specific operations are as follows: Weigh a certain amount of *m*PEG into a three-necked flask containing dry toluene and stir. Weigh a certain molar ratio of *α*-Chloro-*ε*-caprolactone (*α*Cl*ε*CL) and *ε*-Caprolactone (*ε*CL) in a small flask, completely dissolved in a small amount of toluene and added to the reaction vessel. Add three drops of catalyst stannous octoate, under a nitrogen atmosphere, the reaction was heated in a 120 °C oil bath for 12 h. The diblock copolymer *m*PEG-*b*-PCL was obtained. Then, the system was cooled to 60 °C and nitrogen gas was still introduced. The diblock copolymer *m*PEG-*b*-PCL was reacted with Hexamethylene diisocyanate (HMDI) in a ratio of 2:1 for 6 hours, and then the reaction was terminated by cooling, and the product was precipitated with cold methanol. Dissolve in dichloromethane, precipitate with cold diethyl ether, and finally dry in a vacuum oven. The *α*-chloro-*ε*-caprolactone used in this step was synthesized according to the method of the literature [35]. ^{1}H NMR ($CDCl_3$): *δ*-1.68 (m, 3H), *δ*-2.01 (m, 3H), *δ*-4.13 (m, 1H, $COOCH_2$), *δ*-4.53 (m, 1H, $COOCH_2$), *δ*-4.74 (dd, 1H, CHCl).

2.2.2. *Synthesis of* *m*PEG-*b*-[PCL-*g*-(MEO_2MA-*co*-OEGMA)]-*b*-*m*PEG *and azide end-functionalized* *m*PEG-*b*-[PCL-*g*-(MEO_2MA-*co*-OEGMA)]-*b*-*m*PEG

Block-graft copolymer *m*PEG-*b*-[PCL-*g*-(MEO_2MA-*co*-OEGMA)]-*b*-*m*PEG is synthesized by the method of atom transfer radical polymerization (ATRP), and the specific operations are as follows: the triblock copolymer *m*PEG-*b*-PCL-*b*-*m*PEG (412.6 mg, 0.1 mmol) was taken in a dry Schlenk flask with nitrogen gas. The copolymer was completely dissolved with 5 mL of *N*, *N*-dimethylformamide as a reaction solvent. The reaction system was sealed after adding MEO_2MA (1.8 mL, 9.7 mmol) and OEGMA (0.13 mL, 0.3 mmol). The freeze-vacuum-thaw operation is then repeated to remove oxygen from the solution. Then, under continuous nitrogen flow, the catalyst of cuprous chloride (10.3 mg, 0.1 mmol) and the ligand of 2, 2'-bipyridine (31.5 mg, 0.2 mmol) were added to Schlenk tube. After the reaction was heated at 70 °C for 12 hours, the system was cooled. The viscous product was diluted with deionized water and then transferred to a MWCO14kDa dialysis bag for 3 days to remove impurities. After lyophilization, the transparent colloidal product *m*PEG-*b*-[PCL-*g*-(MEO_2MA-*co*-OEGMA)]-*b*-*m*PEG was obtained.

*m*PEG-*b*-[PCL-*g*-(MEO_2MA-*co*-OEGMA)]-*b*-*m*PEG (330 mg), sodium azide (37 mg) were dissolved in *N*, *N*-dimethylformamide, and stir the reaction at room temperature 72 h. The product was precipitated with anhydrous diethyl ether, diluted with water and then transferred to a MWCO14kDa dialysis bag for dialysis for 3 days. After lyophilization, a slightly white colloidal product azide polymer *m*PEG-*b*- [PCL-*g*-(MEO_2MA-*co*-OEGMA)]-*b*-*m*PEG was obtained.

2.2.3. Synthesis of crosslinker alkyne-terminated P(GMA-co-MEO_2MA-co-OEGMA)

P(GMA-*co*-MEO_2MA-*co*-OEGMA) was synthesized by the reversible addition-fragmentation chain transfer polymerization（RAFT）method. First, the chain transfer agent CTA of RAFT was synthesized according to the method in the literature [36]. Passing nitrogen into a dry Schlenk flask, the chain transfer agent CTA (36.4 mg, 0.1 mmol) was dissolved in 5 mL 1,4-dioxane, and then add MEO_2MA (2.5 mL, 13.58 mmol), OEGMA (0.183 mL, 0.42 mmol), GMA (0.082 mL, 0.6 mmol), and finally 20 mg AIBN. The Schlenk flask was placed in a water bath below 10 °C for 40 minutes and then placed in a 60 °C oil bath for reaction. 5 hours later, cooled the reaction system, the product was diluted with deionized water and then transferred to a MWCO14kDa dialysis bag for dialysis for 3 days. After lyophilization, a pale yellow gum product was obtained.

Above P(GMA-*co*-MEO_2MA-*co*-OEGMA) (574 mg) and NaH (46 mg) were completely dissolved in Tetrahydrofuran (THF), stirred for 15 minutes, 166 μL of propargyl bromide was added to the reaction system, and reacted at room temperature for 48 hours. The reaction solution was dialyzed

against a MWCO14kDa dialysis bag for 3 days. After lyophilization, the yellow product alkynylated P(GMA-*co*-MEO$_2$MA-*co*-OEGMA) was obtained.

2.2.4. Synthesis of crosslinker TPOM

TPOM was synthesized according to the methods provided in the previous literature [34]. The specific procedure was as follows: KOH (15.6 g) was thoroughly dissolved in 30 mL of *N*, *N*-dimethylformamide in a dry 100 mL round bottom flask, pentaerythritol (2.5 g) was added, and stirred at 5 °C for 30 minutes. Then, propargyl bromide (20.8 g) was added dropwise to the flask over 20 minutes. The solution was brown and stirred at 40 °C for 24 hours. After adding an appropriate amount of water, the mixture was extracted with 50 mL of diethyl ether. The organic layers were combined, washed with brine and water then dried over anhydrous magnesium sulfate. Finally, an organic solution of ethyl ester:n-hexane (*V*/*V* = 2:8) was used as a mobile phase to purify the column to obtain an orange product.

2.2.5. Preparation of two hydrogels via "click chemistry"

The prepared azided *m*PEG-*b*-[PCL-*g*-(MEO$_2$MA-*co*-OEGMA)]-*b*-*m*PEG and alkynylated P(GMA-*co*-MEO$_2$MA-*co*-OEGMA) in a certain molar ratio dissolved in the deionized water, stirred until the solution was nearly transparent. then, sodium ascorbate (150 mg) was added, stir evenly, and added a few drops of saturated copper sulfate pentahydrate solution quickly, a small amount of gel appeared within 1 min, the reaction was continued at room temperature until present a homogeneous solid gel. The gel was rinsed several times with deionized water to remove unreacted impurities.

The prepared azided *m*PEG-*b*-[PCL-*g*-(MEO$_2$MA-*co*-OEGMA)]-*b*-*m*PEG and the tetrakis (2-propynyloxymethyl)-methane (TPOM) were dissolved in *N*,*N*-dimethylformamide (DMF), *N*, *N*, *N*', *N*', *N*''-pentamethyl diethylenetriamine (PMDETA) (17.4 mg) was added and stirred until the solution was translucent, CuCl (7.2 mg) was quickly added, a small amount of gel appeared within 1 min, and the reaction was continued at room temperature for 24 h.

2.3. Characterization

2.3.1. Nuclear Magnetic Resonance Spectroscopy (^{1}H NMR)

Nuclear magnetic resonance mass spectrometry was performed on a Bruker Avance 300 MHz nuclear magnetic resonance apparatus at room temperature using deuterated chloroform as a solvent.

2.3.2. Fourier Transform Infrared Spectroscopy (FTIR)

The infrared spectrum was measured by a Tensor 27 Fourier transform infrared spectrometer. The sample should be mixed with KBr, ground into a powder and dried before being tableted.

2.3.3. Gel Permeation Chromatography (GPC)

Gel permeation chromatography is a method of characterizing the molecular weight of the copolymer. The method used polystyrene as a standard sample, tetrahydrofuran as a mobile phase, a flow rate of 1 mL/min, and the number average molecular weight (M_n) and polydispersity index (M_w/M_n) were determined by gel permeation chromatography at room temperature.

2.4. Water Solubility and Temperature Sensitivity

The water solubility and temperature sensitivity of the block-graft copolymers were illustrated by digital cameras taking photos of their changes at different temperatures and the transmittance measured by the UV spectrophotometer as a function of temperature.

The preliminary determination of water solubility and temperature sensitivity was carried out by disposing a 2 mg/mL aqueous copolymer solution in a transparent glass vial at room temperature, and after fully stirred, photographed the digital photos at 25 °C, 35 °C and 45 °C respectively.

In addition, the water solubility and temperature sensitivity of the copolymers aqueous solutions were illustrated by measured the transmittance at different temperatures by an ultraviolet spectrophotometer (UV-1901). The transmittance at different temperature of a series of copolymers aqueous solutions with a concentration of 2 mg/mL was measured by UV-visible spectrophotometer and temperature control system, and the correlation curve was drawn according to the change of transmittance with temperature. In the inflection point, the low critical solution temperature (LCST) of the different component block-graft copolymers can be judged. Configured tBG3 aqueous solutions at concentrations of 0.5, 1, 2, 4, 8 mg/mL respectively, and measured the transmittance change of the solutions at 25-50 °C to obtained low critical solution temperature (LCST) of the different concentrations about the tBG3 solutions.

2.5. Micelle Properties of Polymers

Determination of critical micelle concentration (CMC): (1) Determination of critical micelle concentration by surface tension method: prepared a series of copolymer solutions, the surface tension of each copolymer solutions was measured on DCAT21 surface tension meter, and plotted the surface tension as a function of polymer concentration. The turning points were the CMC of the copolymer solutions. (2) Fluorescent probe technology: This method used a certain concentration of pyrene solution, a series of copolymer solutions of different concentrations (10^{-3}~10^{-1}mg/mL), judged the critical micelle concentration (CMC) by a mutation in the I_3/I_1 value after the pyrene is dissolved in the micelle solutions. The measurement was performed with a fluorescence spectrophotometer, and the intensity of the emission spectrum corresponding to I_3 (383 nm) and I_1 (373 nm) at each concentration was recorded. Ploted the I_3/I_1 and log$c$ curves, the turning point was the critical micelle concentration (CMC) of the block-graft copolymer.

The particle size and particle size distribution were measured by dynamic light scattering instrument: configured 1 mg/mL copolymers aqueous solution, and used a water filter with a pore size of 0.45 μm to remove impurities. The particle size of the copolymer aqueous solution in the temperature range of 20-45 °C was measured using a ZS90 type dynamic light scattering instrument.

The micelle morphology was observed by transmission electron microscopy: the copolymers solution with a concentration of 1 mg/mL was prepared, preheated to stability at 25, 35 °C respectively, and the preheated solution was then dropwise to a clean carbon support membrane (200 mesh), after it was naturally dried, it was dyed with 1 wt% of phosphotungstic acid, and dried under vacuum at different temperatures. Finally, samples were prepared by vacuum drying at different temperatures, and the micelle morphology was observed by a JEM-2100 transmission electron microscope.

2.6. Sol-Gel Transition

Dispensed polymer solutions of different mass concentrations in vials, stirred them evenly, placed each polymer solution in a 20 °C - 50 °C water bath until the solution was equilibrated, each rising temperature is 2 °C. After balance, observed and recorded the state of the copolymer solutions.

2. 7. SEM Analysis of Gel

The two different gels synthesized were fully swelled in water, and then freeze-dried to obtain dry gels, and the surface morphology of the two dry hydrogels was taken by a uniform scanning cross section in an environmental scanning electron microscope.

3. Results and Discussion

3.1. Synthesis and Characterization of tBG Copolymer and Hydrogels

In this study, the diblock copolymer *m*PEG-*b*-PCL was synthesized by ring-opening reaction of ε-caprolactone and *m*PEG, and $Sn(Oct)_2$ as catalyst. The reaction was continued under the action of the coupling agent HMDI to couple the *m*PEG-*b*-PCL to synthesize the *m*PEG-*b*-PCL-*b*-*m*PEG triblock copolymer. Then, the P(MEO_2MA-*co*-OEGMA) was grafted into the side chain of *m*PEG-*b*-PCL-*b*-*m*PEG triblock copolymer by ATRP, the *m*PEG-*b*-[PCL-*g*-(MEO_2MA-*co*-OEGMA)] -*b*-*m*PEG triblock-graft copolymer was synthesized, and azide end-functionalized the triblock-graft copolymer. Under the premise of synthesizing the triblock-graft copolymer, the crosslinker alkynyl P(GMA-*co*-MEO_2MA-*co*-OEGMA) was synthesized by RAFT, and another crosslinker agent TPOM was synthesized by organic reaction. Finally, the azided triblock-graft copolymer was chemically clicked separately with the two crosslinkers under different conditions to form a hydrogel. As shown in **Scheme 1**.

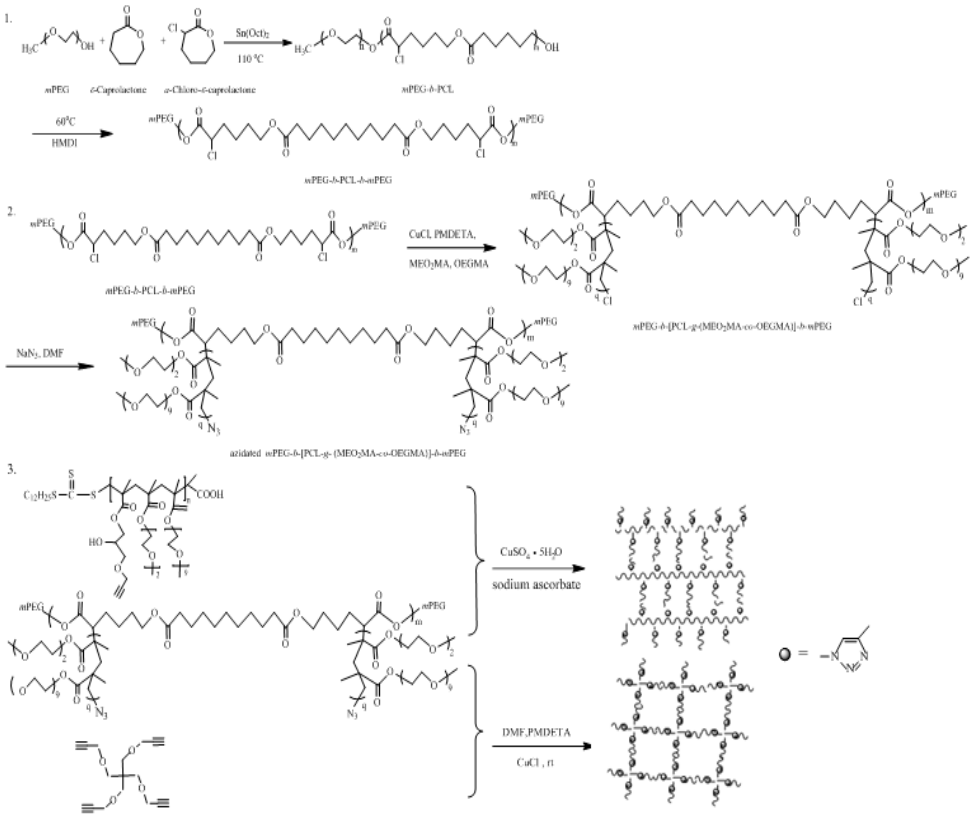

Scheme 1. Synthesis of copolymer *m*PEG-*b*-[PCL-*g*-(MEO_2MA-*co*-OEGMA)]-*b*-*m*PEG and preparation of two hydrogels.

The chemical structure of the *m*PEG-*b*-PCL-*b*-*m*PEG triblock copolymer, the *m*PEG-*b*-[PCL-*g*-(MEO_2MA-*co*-OEGMA)]-*b*-*m*PEG triblock-graft (tBG) copolymer and the azide end-functionalized *m*PEG-*b*-[PCL-*g*-(MEO_2MA-*co*-OEGMA)]-*b*-*m*PEG copolymer were demonstrated by nuclear magnetic resonance mass spectrometry and Fourier transform infrared spectroscopy. **Figure S1** is the nuclear magnetic spectrum of *m*PEG-*b*-PCL-*b*-*m*PEG triblock copolymer and *m*PEG-*b*- [PCL-*g*-(MEO_2MA-*co*-OEGMA)]-*b*-*m*PEG triblock-graft copolymer. In **Figure S1 (a)**, 3.59 and 3.31 ppm are representative peaks of hydrogen atoms in the $-CH_2CH_2O-$ and $-OCH_3$ groups in *m*PEG. 4.00, 2.24, 1.55 and 1.31 ppm are representative peaks of hydrogen atoms in $-CH_2OOC-$, $-OCCH_2-$ and $-(CH_2)_3-$ in PCL respectively. There is a very weak peak at 4.10 ppm, which represents the methyl proton peak of -OCCHCl. In **Figure S1 (b)**, the proton peak at 4.10 ppm of -OCCHCl disappears, and the resonance

peaks of hydrogen in -CH_2OOC-, -OCH_2CH_2O- and -OCH_3 of the graft chain P(MEO_2MA-*co*-OEGMA) have respectively appeared at 4.03, 3.55 and 3.31 ppm. Figures S1(a) and S1(b) illustrate the block-graft copolymers synthesied successfully. **Figure S2** is infrared spectrum of the *m*PEG-*b*-[PCL-*g*-(MEO_2MA-*co*-OEGMA)]-*b*-*m*PEG triblock-graft copolymer and the azide end-functionalized *m*PEG-*b*-[PCL-*g*-(MEO_2MA-*co*-OEGMA)]-*b*-*m*PEG triblock-graft copolymer. In this figure, near the 1700 cm^{-1} is a C=O stretching vibration peak. Comparing **Figure S2 (a)** and **Figure S2 (b)**, the peak at 2097 cm^{-1} is the characteristic absorption position of -N_3, indicating that the azide group is successfully connected to the copolymer chain.

Figure S3 is the nuclear magnetic spectrum of the RAFT chain transfer agent CTA and the P(GMA-*co*-MEO_2MA-*co*-OEGMA). The resonance peaks of CTA are 0.82, 1.184, 1.67 and 3.2 ppm, which corresponding to the proton on the -CH_3, -$(CH_2)_9$-, -CH_2- and -CCH_3, and -CH_2S- groups respectively. The presence of these peaks indicates CTA synthesized successfully [36]. The peaks near 1.24 and 1.83 ppm in the nuclear magnetic spectrum below is respective corresponding to the -$CH(CH_3)_2$ and -CH_2- groups on the main chain. The peaks at 3.376, 3.624 and 4.10 ppm are corresponding to the proton of the -OCH_3, -CH_2O- and -$COOCH_2$- groups on the branches, respectively. It was proved that P(GMA-*co*-MEO_2MA-*co*-OEGMA) was also successfully prepared. **Figure S4** is infrared spectra of P(GMA-*co*- MEO_2MA-*co*-OEGMA) and alkynylated P(GMA-*co*-MEO_2MA-*co*-OEGMA). Comparing the two figures, an obvious alkynyl characteristic absorption peak appeared at 2063 cm^{-1} in the infrared spectrum below, indicating that the alkynylated P(GMA-*co*-MEO_2MA-*co*-OEGMA) was successfully synthesized.

Figure S5 shows the infrared spectrum of the azided triblock-graft copolymer, the crosslinker alkynylated P(GMA-*co*-MEO_2MA-*co*-OEGMA), the crosslinker TPOM and the two gels. **Figure S5(a)** same with **Figure S2(b)**, is the infrared spectrum of the azided triblock-graft copolymer. **Figure S5(b)** represents the crosslinker alkynylated P(GMA-*co*-MEO_2MA-*co*-OEGMA). **Figure S5(c)** is the infrared spectrum of TPOM, the peaks at 3280 cm^{-1} show the existence of the C≡CH. **Figure S5(d)** and **S5(e)** represent the infrared spectrum of the two gels respectively. Observed the **Figure S4**, the infrared spectrum of gels no longer shows the characteristic functional groups of the reactants of the crosslinkers, indicating that the azided triblock-graft copolymer reacts well with both crosslinkers.

In the step of *m*PEG-*b*-PCL-*b*-*m*PEG triblock copolymer synthesis, the total amount of *ε*-Caprolactone and *α*-Chloro-*ε*-Caprolactone added to the reaction remained unchanged, while the ratios of the *ε*-Caprolactone and the *α*-Chloro-*ε*-Caprolactone were respectively 8:2, 7:3, 6:4, 5:5. The difference in the content of the characteristic functional group CL determines the difference in the total amount of the grafted MEO_2MA and OEGMA copolymer on the triblock-graft copolymer. Therefore, the molecular weight of the copolymers also differs. The molecular weight of each polymer was measured by gel permeation chromatography as shown in **Table S1**. The measured molecular weight of the polymer is consistent with the molecular weight of the experimental design basically. At the same time, the measured PDI values are less than 1.20, indicating that the method used in the experiment is indeed advantageous for the synthesis of polymers with narrow molecular weight distribution.

3.2. Water solubility and temperature sensitivity

The length of the hydrophilic *m*PEG segment in the triblock copolymers *m*PEG-*b*-PCL-*b*-*m*PEG is limited, and the hydrophobic PCL chain determines that the water solubility of the polymer is relatively poor [30]. The triblock copolymers *m*PEG-*b*-PCL-*b*-*m*PEG was added in deionized water and did not solved. The water solubility of the triblock-graft copolymer *m*PEG-*b*-[PCL-*g*- (MEO_2MA-*co*-OEGMA)]-*b*-*m*PEG is greatly improved due to the P(MEO_2MA-*co*-OEGMA) graft chains. This is because the hydrophilic oligo (ethylene glycol) graft chain in P(MEO_2MA -*co*-OEGMA) forms a hydrogen bond with the solvent water molecule. In addition, the PEG analogues polymer formed by the polymerization of MEO_2MA and OEGMA also has unique temperature sensitivity. Therefore, these two substances give the copolymer of corresponding temperature sensitivity [31]. **Figure 1** is a photograph of the triblock-graft copolymers (tBG) at 25 °C, 35 °C and 45 °C. The tBGs solution at 25 °C is clear, and with the temperature rises, the tBGs solution gradually cloudy.

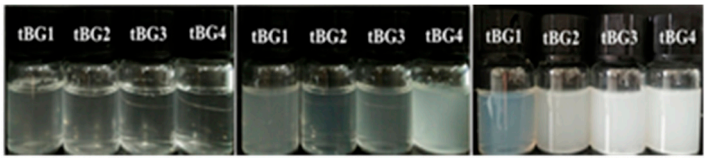

Figure 1. Photographs of the block-graft copolymers aqueous solutions (2 mg/mL) at 25 °C, 35 °C and 45 °C.

The specific case is illustrated by the transmittance curve measured by an ultraviolet spectrophotometer. As shown in **Figure 2(a)**, the transmittance of the tBG1 to tBG4 solution gradually increases at room temperature because the density of the characteristic functional group Cl of the tBG1 to tBG4 is increased with the same polymerization degree. That is, from tBG1 to tBG4, the water-soluble improved according to the increased density of the copolymer P(MEO_2MA-*co*- OEGMA) segment in the graft, so the solution becomes more and more transparent. In addition, as can be seen from the figure, the transmittance of the four copolymer aqueous solutions began to decrease sharply after 35 °C, indicating that the LCST of the tBGs solutions is 35 °C. After 40 °C, the transmittance of tBG1 was almost no longer decreased, and the transmittance of the others solution was 0%, indicating that the same concentration of the polymer aqueous solution, the content of MEO_2MA and OEGMA is one of the important factors that affect the temperature sensitivity of the copolymer.

Figure 2(b) is a graph showing the transmittance with different concentration of the tBG3 aqueous solutions as a function of temperature, and **Figure 2(c)** is the LCST curve with different concentration of the tBG3 aqueous solution. Combining the two graphs, it can be seen that the LCST of the same copolymer solution gradually decreases as the concentration increases from 1 mg/mL to 8 mg/mL. This shows that the choice of concentration is also very important when studying copolymer solution, whether the concentration is too high or too low, it affects the normal function of its action.

3.3. Critical Micellization Concentration Determination (CMC)

The copolymer molecules are present in a single molecule state when the concentration of the amphiphilic copolymer solution is very low. As the concentration of the copolymer solution increases to a certain value, the copolymer molecules self-assemble to form nanoscale core-shell micelles, this concentration value is the critical micelle concentration of the copolymer solution. There are many methods for determining the critical micelle concentration. In this study, two experimental methods were used to determining the critical micelle concentration: fluorescence spectrometer and surface tension meter.

Figure 3 (a) shows the CMC of the tB2 solution is 0.0047 mg/mL, **Figure 3(b)** shows that the CMC of tBG2, tBG3, and tBG4 solutions are 0.0237 mg/mL, 0.0599 mg/mL, and 0.0841 mg/mL respectively, and these values are several to ten times greater than the CMC of the tB2 solution. This is because the addition of the hydrophilic segment of P(MEO_2MA-*co*-OEGMA) makes it impossible for the copolymer solution which can balance the hydrophilic-hydrophobic chain to form micelles at the original critical micelle concentration, and the hydrophilic segment is slightly superior. In this case, a greater concentration is required to achieve a new hydrophilic-hydrophobic chain balance to form micelles. That is, the larger the amount of the hydrophilic chain P(MEO_2MA-*co*-OEGMA) added, the larger the CMC of the formed block-graft copolymer [37,38].

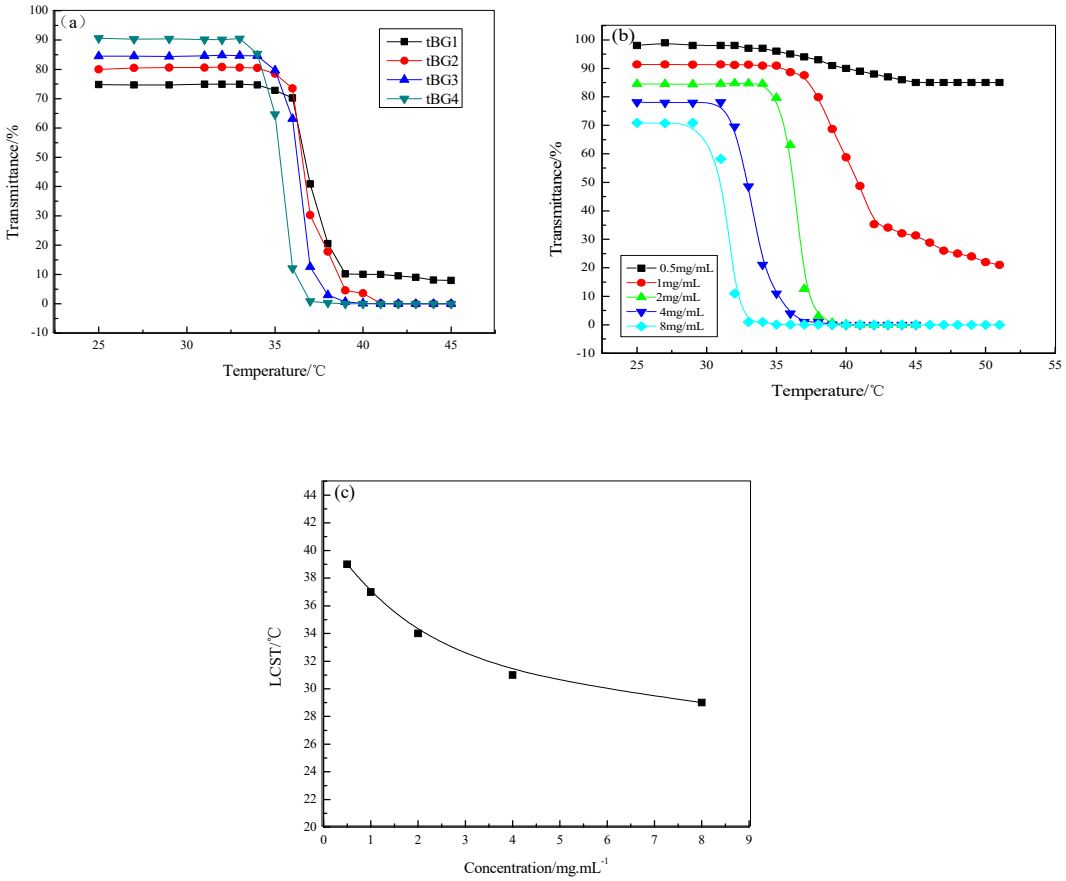

Figure 2. The transmittance of the tBG1 to tBG4 aqueous solution (a), the transmittance with different concentration of the tBG3 aqueous solution (b), and the LCST curve with different concentration of the tBG3 aqueous solution (c).

Figure 3(c) is a graph showing the surface tension in different concentrations of tBG3 and tBG4 copolymers solutions measured by the surface tension method, and the turning point is the CMC of the copolymers. Before the turning point, the surface tension decreases rapidly with the increase of the solution concentration. When reaching the CMC, the copolymer self-assembly forms micelles in the solution. After the CMC, the surface tension hardly changes with the increase of the solution concentration. The results measured by this method are close to the CMC measured by the fluorescent probe method, and the CMC of the tBG4 solution is greater than the CMC of the tBG3 solution under the same conditions, too. It also demonstrates that under certain conditions, the better hydrophilicity of the copolymer is the larger CMC is

Preprints (www.preprints.org) | NOT PEER-REVIEWED | Posted: 14 March 2019 doi:10.20944/preprints201903.0151.v1

Peer-reviewed version available at Polymers 2019, 11, 765; doi:10.3390/polym11050765

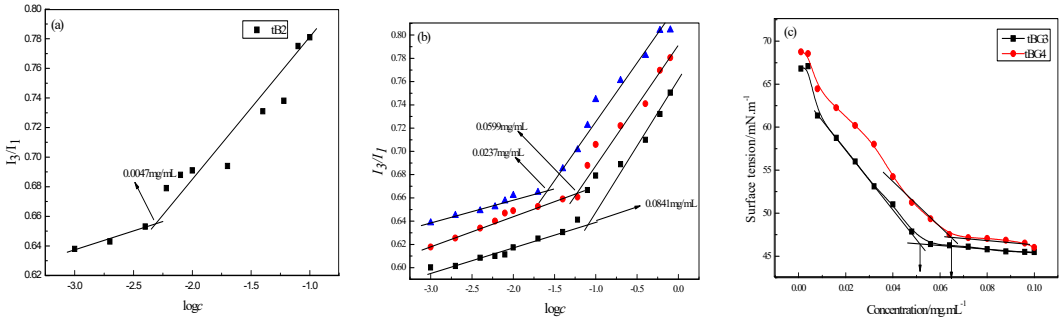

Figure 3. The CMC of the copolymer tB2 (a), the CMC of copolymer tBG2, tBG3, and tBG4 measured by fluorescence spectrometer (b), and the CMC of copolymers tBG3 and tBG4 measured by the surface tension method (c).

3.4. Particle Size of Copolymer Micelles

Figure 4 (a) is the graph showing the particle size distribution measured by the dynamic light scattering instrument at room temperature for the four-component copolymers micelles of tBG1 to tBG4. It can be seen from the figure that the particle size of the four groups of copolymers is very small under the same conditions, and they are centralized at 60～70 nm. At the same time, as the density of the graft chain P(MEO_2MA-*co*-OEGMA) increases from tBG1 to tBG4, the micelle particle size distribution range slightly expands. This is probably because small particle size micelles are produced due to polymerization unevenness during the synthesis [39].

Figure 4 (b) shows the particle size distribution of the tBG4 copolymer micelles solution at 25 °C and 37 °C. It can be seen that the particle size of the micelles is mainly distributed around 60 nm at 25 °C, and with the temperature increases to 37 °C, the particle size of the micelles also increases to about 200 nm. The reason about the particle size of micelles in tBG4 copolymer solution increases with temperature is that the hydrophobic PCL chain in the tBG4 block-graft copolymer forms the core of the micelle, hydrophilic PEG and P(MEO_2MA-*co*-OEGMA) chains form the shell of the micelle, but the graft chain P(MEO_2MA-*co*-OEGMA) forms hydrogen bonds with water molecules at 25 °C [40], which lead the graft chain in an extended state, and the actual particle size is equivalent to being formed only by the backbone PCL-PEG. While as the temperature reaches 37 °C, the hydrogen bonding of the graft chain P(MEO_2MA-*co*-OEGMA) and water molecules becomes weak, and the P(MEO_2MA-*co*-OEGMA) chain begins to collapse outside the original small particle size micelles, at this time, a large amount of P(MEO_2MA-*co*-OEGMA) graft chain adhered to the micelle core, and the particle size of the entire micelle increased a lot [33].

Transmission electron microscopy is one of the most common methods for studying the morphology of copolymer micelles. This method can not only clearly observe the morphology of the micelles, but also measure the particle size of the micelles. In order to more intuitively introduce the micelles formed by the self-assembly in the copolymer aqueous solution, taken tBG4 as an example, the transmission electron micrographs of the tBG4 copolymer micelles measured at 25 °C and 37 °C, as shown in **Figure 4 (c)**. The morphology of the micelles formed by the copolymer can be clearly seen from the figure. The copolymer aqueous solution is very homogeneous at 25 °C, therefore，the prepared micelles are evenly dispersed on the copper mesh. In this situation, the particle diameter of the micelle was about 50 nm. When the copolymer aqueous solution was preheated to 37 °C, the hydrogen bond between the graft chain P(MEO_2MA-*co*-OEGMA) and the water molecules began to be destroyed, the copolymer aqueous solution was not as uniform as at 25 °C, and began to become cloudy. The micelles sample prepared in this case can be observed the larger particle size, but these micelles no longer a regular spherical shape and the particle diameter of the micelles were 160 nm. Comparing Figure 4 (a) with Figure 4 (b), it can be found that the particle size of the micelles measured by the dynamic light scattering instrument is slightly larger than the micelles diameter observed by the transmission electron microscope, it is because the particle size measured by the dynamic light scattering is directly measured the micelles in the aqueous solution, the entire

molecular group is relatively stretched, but the particle size measured by the transmission electron microscope is the dry copolymer solution obtained by dropping the copolymer solution on a copper mesh and drying it.

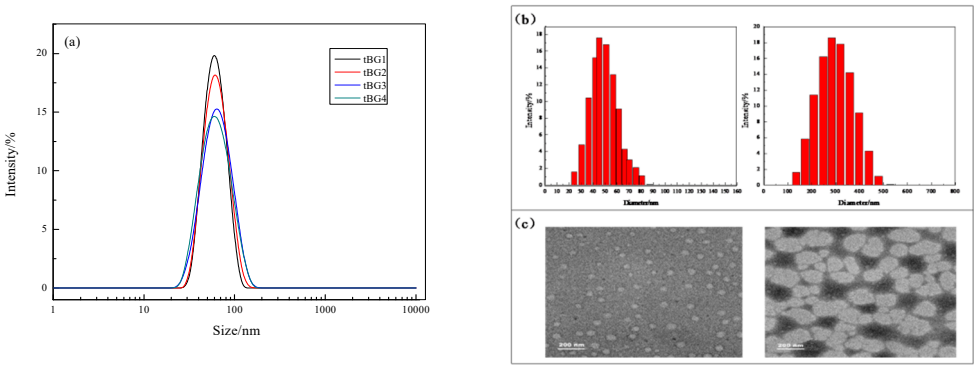

Figure 4. Size distributions of tBGs aqueous solutions (a), measured by DLS at 25 °C and 37 °C (b), TEM images of tBG4 micelles at 25 °C and 37 °C (c).

3.5. Sol-Gel Transition

Figure 5(a) recorded the sol-gel transition of the different concentrations of the tBG3 copolymer aqueous solution. It can be seen from the Figure that the sample solution is still in a flowing state before 25 °C. After the temperature has risen to 30 °C, the highest concentration copolymer aqueous solution with the 25% (wt) has formed a gel, and inverted the vial for 1 min, the gel just flow a slight. Subsequently, 15% (wt) and 20% (wt) of the copolymer aqueous solution have also converted into a gel at 35 °C, while 10% (wt) of the polymer solution is dehydrated directly, and appears white flocculent substance. As the temperature continues to rise, each component copolymer gels begin to dehydrate. This process illustrates that the sol-gel transition temperature of the copolymer aqueous solution decreases with the increasing of the concentration.

Figure 5(b) is the sol-gel transition phase diagram, plotted from the copolymers aqueous solution state change according to the temperature. In order to directly show the effect that the concentration of the copolymer aqueous solution on the sol-gel transition temperature. When the concentration of the polymer solution reaches a certain level, the amount of micelles in the copolymer aqueous solution is also very large, the branches out the core-shell structure of micelles are in contact with each other, forming a plurality of crosslinking points which can be crosslinked to constitute the gel. The greater the concentration of the copolymers aqueous solution is, the more crosslinking points provided are, and at the same time, the lower the induced temperature is. After the copolymer aqueous solution transformed into a gel by temperature induction, as the temperature continues to increase, the graft chains of copolymer micelle collapsed and the dehydration in the core is intensified, the cross-linking point is destroyed, and the collapsed dehydrated micelles is partially viscous, the water is separated out of the micelle and the copolymer aqueous solution is converted from the gel state to white floc.

The conversion of the polymer solution from the sol to the gel is based on the cross-linking point formed by the weak interaction between the outer branches of the micelle core, it is a physical cross-linking, so the sol-gel transition process is reversible, the copolymer aqueous solution can achieve a reversible transformation of the sol-gel depending on the rise and fall of the temperature [41]. As shown in **Figure 5(c)**.

3.6. SEM Analysis of Gel

The morphology of the two dry gels observed under a scanning electron microscope is shown in the **Figure 6**. Both gels have the relatively obvious network structure. **Figure 6(a)** and **Figure 6(b)** are scanned photographs of the gel formed by the azide block-graft copolymer and the crosslinker alkynyl P(MEO_2MA-*co*- OEGMA) at 25 °C and 40 °C respectively. The network has a slightly thick

hole wall and the structure is relatively incomplete. It is possible that the insufficient reaction between the azide block-graft copolymer with the alkynyl P(MEO$_2$MA-*co*-OEGMA). **Figure 6(c)** and **Figure 6(d)** are scanned photographs of the gel formed by the azide block-graft copolymer and the crosslinker TPOM at 25 °C and 40 °C respectively. The network structure is relatively complete and the pore walls are thin. Comparing the changes of the two gels at 25 °C and 40 °C, it can be seen that the gel is in a shrinking state at 40 °C, and the three-dimensional network pore size becomes smaller. This also verifies that both gels are temperature sensitive.

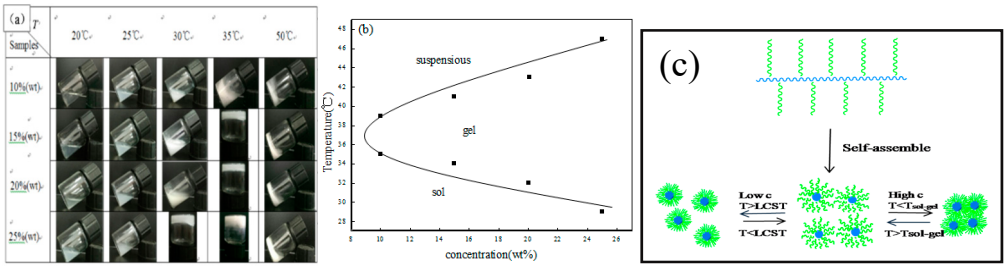

Figure 5. Photographs of the different concentrations tBG3 copolymer aqueous solution at different temperature (a), the sol-gel transition phase diagram of tBG3 (b), and schematic representation of the self-assembled thermo-sensitive core-shell micelles (c).

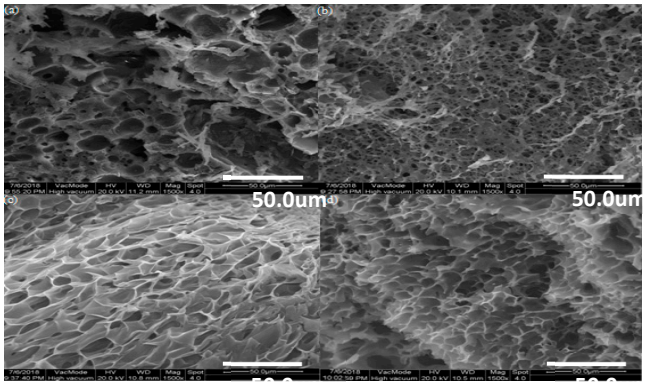

Figure 6. The morphology of gel1 at 25 °C (a) and 40 °C (b), the morphology of gel2 at 25 °C (c) and 40 °C (d).

4. Conclusions

The novel hydrogel is composed of the block-graft copolymer *m*PEG-*b*-[PCL-*g*-(MEO$_2$MA -*co*-OEGMA)]-*b*-*m*PEG with the alkynyl P(GMA-*co*-MEO$_2$MA-*co*-OEGMA) and TPOM by click chemistry. The water-soluble and temperature sensitive block-graft copolymer *m*PEG-*b*-[PCL-*g*-(MEO$_2$MA-*co*-OEGMA)]-*b*-*m*PEG was synthesized by ROP and ATRP. While the alkynyl P(GMA-*co*-MEO$_2$MA-*co*-OEGMA) synthesized by RAFT also has good water solubility and temperature sensitivity. The LCST of the block-graft copolymer is designed within the normal physiological temperature of the human body. The results of dynamic light scattering and transmission electron microscopy specifically show that the trend of micelle particle size increases first and then decreases with temperature increases. The azide *m*PEG-*b*-[PCL-*g*-(MEO$_2$MA-*co*- OEGMA)]-*b*-*m*PEG molecules react with the crosslinker to form the gel via click chemistry. The internal three-dimensional network morphology of the gel measured by scanning electron microscopy at different temperatures certified that the hydrogel has temperature sensitivity.

Supplementary Materials: The following are available online at www.mdpi.com/link. Figure S1: ^{1}HNMR spectra of *m*PEG-*b*-PCL-*b*-*m*PEG triblock copolymer and *m*PEG-*b*-[PCL-*g*-(MEO$_2$MA-*co*-OEGMA)]-*b*-*m*PEG block-graft copolymer, Figure S2: FT-IR spectra of *m*PEG-*b*-[PCL-*g*-(MEO$_2$MA-*co*-OEGMA)]-*b*-*m*PEG block-graft copolymer and diazide end-functionalized *m*PEG-*b*-[PCL-*g*-(MEO$_2$MA-*co*-OEGMA-*b*-*m*PEG block-graft

copolymer, Figure S3: ^{1}HNMR spectra of CTA and P(GMA-*co*-MEO$_2$MA-*co*-OEGMA), Figure S4: FT-IR spectra of P(GMA-*co*-MEO$_2$MA-*co*-OEGMA) and alkynylated P(GMA-*co*-MEO$_2$MA-*co*-OEGMA), Figure S5: FT-IR spectra of the azidized block-graft copolymer, the crosslinker alkynylation P(GMA-*co*- MEO$_2$MA-*co*-OEGMA), the crosslinker TPOM and the two gels, Table S1: Characterization of various copolymers

Figure S1 ^{1}HNMR spectra of the triblock copolymer *m*PEG-*b*-PCL-*b*-*m*PEG (a) and triblock- graft copolymer *m*PEG-*b*-[PCL-*g*-(MEO$_2$MA-*co*-OEGMA)]-*b*-*m*PEG (b)

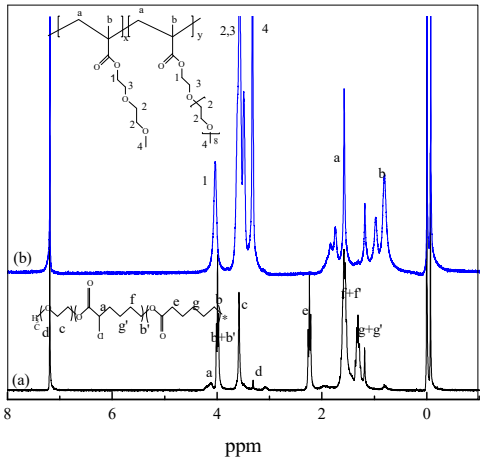

Figure S2 FT-IR spectra of *m*PEG-*b*-[PCL-*g*-(MEO$_2$MA-*co*-OEGMA)]-*b*-*m*PEG triblock-graft copolymer (a) and azide *m*PEG-*b*-[PCL-*g*-(MEO$_2$MA-*co*-OEGMA-*b*-*m*PEG triblock-graft copolymer (b)

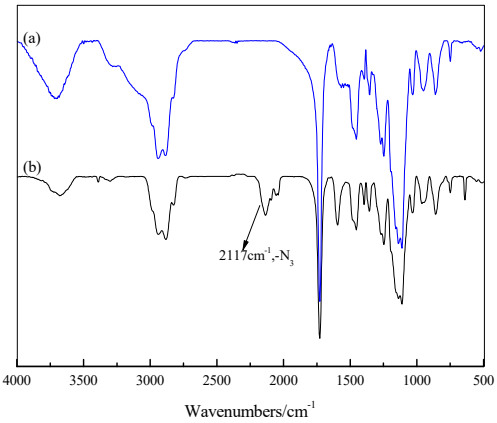

Figure S3 ^{1}HNMR spectra of CTA (a) and P(GMA-*co*-MEO$_2$MA-*co*-OEGMA) (b).

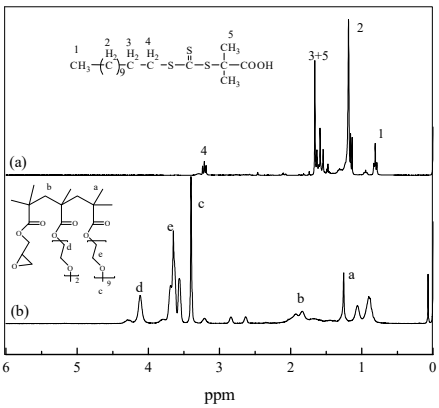

Figure S4 FT-IR spectra of P(GMA-*co*-MEO$_2$MA-*co*-OEGMA) and alkynyl P(GMA-*co*- MEO$_2$MA-*co*-OEGMA).

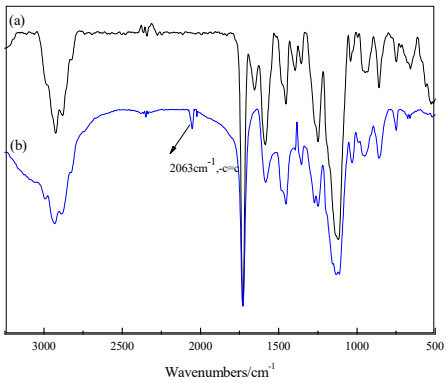

Figure S5 FT-IR spectra of the azide triblock-graft copolymer (a), the crosslinker alkynyl P(GMA-*co*-MEO$_2$MA-*co*-OEGMA) (b), the crosslinker TPOM (c) and the two gels (d, e).

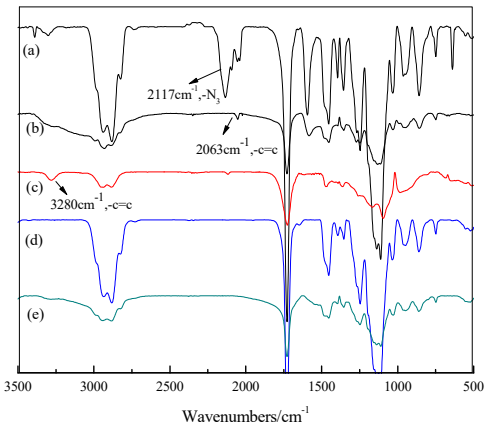

Table S1: Characterization of copolymers

Table S1 Characterization of various copolymers

Samples	[αClεCL]/[εCL][a] (n:n)	[αClεCL]/[MO][b] (n:n)	$M_{n,}$ theory[c] (g/mol^{-1})	GPC results	
				M_n (g/mol^{-1})[d]	PDI[e]
tB1	2:8		3920	4132	1.072
tB2	3:7		3988	4184	1.044
tB3	4:6		4057	4349	1.021
tB4	5:5		4126	4435	1.089
tBG1	2:8	1:10	30448	32506	1.102
tBG2	3:7	1:10	39793	46822	1.098
tBG3	4:6	1:10	53058	57408	1.114
tBG4	5:5	1:10	66322	68261	1.158

tB1, tB2, tB3, and tB4 represent the triblock copolymer *m*PEG-*b*-PCL-*b*-*m*PEG. tBG1 tBG2, tBG3, and tBG4 represent the triblock-graft copolymer *m*PEG-*b*-[PCL-*g*-(MEO$_2$MA-*co*-OEGMA)]-*b*-*m*PEG. [MO][b] is the initial molar ratio of MEO$_2$MA and OEGMA, the ratio between MEO$_2$MA and OEGMA in all block-graft copolymers is 97:3.

Acknowledgments: This research was supported by the National Natural Science Foundation of China (No. 21773147) and the Natural Science Foundation of Shaanxi Province of China (No. 2016JM2003).

Author Contributions: Shouxin Liu and Pei Shang conceived and designed the experiments; Pei Shang, Jie Wu, Xiaoyu Shi, Zhidan Wang and Fei Song performed the experiments and analyzed the data; Pei Shang and Shouxin Liu provided additional intellectual insight and prepared the manuscript.

Conflicts of Interest: The authors declare no conflict of interest.

References

1. Yuan, Y.; Zhang, A.K.; Ling, J.; Yin, L.H.; Chen, Y.; Fu, G.D. Well-defined biodegradable amphiphilic conetworks. *Soft Matter* **2013**, *9*, 6309–6318.
2. Li, L.; Lu, B.B.; Wu, J.N.; Fan, Q.K.; Guo, X.H.; Liu, Z.Y.; Synthesis and self-assembly behavior of thermo-responsive star-shaped POSS-(PCL- P(MEO$_2$MA-*co*-PEGMA))$_{16}$ inorganic/organic hybrid block copolymers with tunable lower critical solution temperature. *New J. Chem.* **2016**, *40*, 4761–4768.
3. Han, Y.; Li, Y.H.; Zeng, Q.Y.; Li, H.Y.; Peng, J.L.; Xu, Y.H.; Chang, J. Injectable bioactive akermanite/alginate composite hydrogels for in situ skin tissue engineering. *J. Mater. Chem. B* **2017**, *5*, 3315–3326.
4. Döring, A.; Birnbaum, W.G.; Kuckling, D. Responsive hydrogels-structurally and dimensionally optimized smart frameworks for applications in catalysis, micro-system technology and material science. *Chem. Soc. Rev.* **2013**, *42*, 7391–7420.
5. Lin, G.Y.; Cosimbescu, L.; Karin, N.J.; Gutowska, A.; Tarasevich, B.J. Injectable and thermogelling hydrogels of PCL-*g*-PEG: mechanisms, rheological and enzymatic degradation properties. *J. Mater. Chem. B* **2013**, *1*, 1249–1255.
6. Kabir, M.H.; Hazama, T.; Watanabe, Y.; Gong, J.; Murase, K.; Suanda, T.; Furukawa, H. Smart hydrogel with shape memory for biomedical applications. *Journal of the Taiwan Institute of Chemical Engineers.* **2014**, *45*, 3134–3138.
7. Lim, H.L; Hwang, Y.S; Kar, M.; Varghese, S. Smart hydrogels as functional biomimetic systems. *Biomater. Sci.* **2014**, *2*, 603–618.
8. Yu. L.; Ding, J.D. Injectable hydrogels as unique biomedical materials. *Chem. Soc. Rev.* **2008**, *37*, 1473–1481.
9. Ravichandran, R.; Astrand, C.; Patra, H.K.; Turner, A.P.F.; Chotteau, V.; Phopase, J. Intelligent ECM mimetic injectable scaffolds based on functional collagen building blocks for tissue engineering and biomedical applications. *RSC Adv.* **2017**, *7*, 21068–21078.
10. Che, Y.J.; Li, D.P.; Liu, Y.L.; Ma, Q.L.; Tan, Y.B.; Yue, Q.Y.; Meng, F.J. Physically cross-linked pH-responsive chitosan-based hydrogels with enhanced mechanical performance for controlled drug delivery. *RSC Adv.* **2016**, *6*, 106035–106045.

11. Ding, X.C.; Wang, Y.D. Weak bond-based injectable and stimuli responsive hydrogels for biomedical applications. *J. Mater. Chem. B* **2017**, *5*, 887-906.
12. Gong, Z.Y.; Zhang, G.P.; Zeng, X.L.; Li, J.H.; Li, G.; Huang, W.P.; Sun, R.; Wong, C.P. High-strength, tough, fatigue resistant, and self-healing hydrogel based on dual physically cross-linked network. *ACS Appl. Mater. Interfaces* **2016**, *8*, 24030−24037.
13. Qian, S.S.; Zhou, C.; Xu, L.Q.; Yao, F.; Cen, L.; Fu, G.D. High strength biocompatible PEG single-network hydrogels. *RSC Adv.* **2014**, *4*, 25241−25250.
14. Kolb, H.C.; Finn, M.G.; Sharpless, K.B. Click chemistry: diverse chemical function from a few good reactions. *Angew. Chem. Int. Ed.* **2001**, *40*, 2004−2021.
15. Es-haghi, S.S.; Leonov, A.I.; Weiss, R.A. Deconstructing the double-network hydrogels: the importance of grafted chains for achieving toughness. *Macromolecules* **2014**, *47*, 4769−4777.
16. Hemingway, M.G.; Gupta, R.B.; Elton, D.J. Hydrogel nanopowder production by inverse-miniemulsion polymerization and supercritical drying. *Ind. Eng. Chem. Res.* **2010,** *49*, 10094–10099.
17. Malkoch, M.; Vestberg, R.; Gupta, N.; Mespouille, L.; Dubois, P.; Mason, A.F.; Hedrick, J.L.; Liao, Q.; Frank, C.W.; Kingsbury, K.; Hawker, C.J. Synthesis of well-defined hydrogel networks using click chemistry. *Chem. Commun.* **2006**, 2774–2776.
18. Crescenzi, V.; Cornelio, L.; Meo, C.D.; Nardecchia, S.; Lamanna, R. Novel hydrogels via click chemistry: synthesis and potential biomedical applications. *Biomacromolecules* **2007**, *8*, 1844–1850.
19. Ossipov, D.A.; Hilborn, J. Poly(vinyl alcohol)-based hydrogels formed by "click chemistry". *Macromolecules* **2006**, *39*, 1709–1718.
20. Grover, G.N.; Lam, J.; Nguyen, T.H.; Segura, T.; Maynard, H.D. Bicompatible hydrogels by oxime click chemistry. *Biomacromolecules* **2012**, *13*, 3013–3017.
21. Meldal, M.; Tornøe, C.W. Cu-catalyzed azide-alkyne cycloaddition. *Chem. Rev.* **2008**, *108*, 2592−3015.
22. Chang, L.L.; Deng, L.D.; Wang, W.W.; Lv, Z.S.; Hu, F.Q.; Dong, A.J.; Zhang, J.H. Poly(ethyleneglycol)-*b*-Poly(ε-caprolactone-*co*-γ-hydroxyl-ε-caprolactone) bearing pendant hydroxyl groups as nanocarriers for doxorubicin delivery. *Biomacromolecules* **2012**, *13*, 3301−3310.
23. Thévenaz, D.C.; Monnier, C.A.; Balog, S.; Fiore, G.L. Luminescent nanoparticles with lanthanide-containing poly(ethylene glycol)-poly(ε-caprolactone) block copolymers. *Biomacromolecules* **2014**, *15*, 3994−4001.
24. Vidyasagar, A.; Ku, S.H.; Kim, M.; Kim, M.; Lee, H.S.; Pearce, T.R.; McCormick, A.V.; Bates, F.S.; Kokkoli, E. Design and characterization of a PVLA-PEG-PVLA thermosensitive and biodegradable hydrogel. *ACS Macro Lett.* **2017**, *6*, 1134−1139.
25. Chandel, A.K.S.; Kumar, C.U.; Jewrajka, S.K. Effect of polyethylene glycol on properties and drug encapsulation−release performance of biodegradable/ cytocompatible agarose−polyethylene glycol−polycaprolactone amphiphilic co-network gels. *ACS Appl. Mater. Interfacs* **2016**, *8*, 3182−3192.
26. He, J.P.; Chen, J.Z.; Lin, S.L.; Niu, D.C.; Hao, J.; Jia, X.B.; Li, N.; Gu, J.L.; Li, Y.S.; Shi, J.L. Synthesis of a pillar[5]arene-based polyrotaxane for enhancing the drug loading capacity of PCL-based supramolecular amphiphile as an excellent drug delivery platform. *Biomacromolecules* **2018**, *19*, 2923−2930.
27. Jain, E.; Hill, L.; Canning, E.; Sell, S.A.; Zustiak, S.P. Control of gelation, degradation and physical properties of polyethylene glycol hydrogels through the chemical and physical identity of the crosslinker. *J. Mater. Chem. B* **2017**, *5*, 2679−2691.
28. Blackwell, C.J.; Haernvall, K.; Guebitz, G.M.; Groombridge, M. ; Gonzales, D.; Khosravi, E. Enzymatic degradation of star poly(ε-caprolactone) with different central units. *Polymers.* **2018**, *10,* 1266.
29. Liu, S.X.; Li, X.; Guang, N.E.; Tian, L.; Mao, H.G.; Ning, W.Y. Novel amphiphilic temperature responsive graft copolymers PCL-*g*-P(MEO_2MA-*co*- OEGME) via a combination of ROP and ATRP: synthesis, characterization, and sol-gel transition. *J. Polym. Res.* **2016**, *23*, 141−153.
30. Wang, Q.Q.; Liu, S.X.; Sheng, W.J.; Guang, N.E.; Li, X. Synthesis and sol-gel transition of novel temperature responsive ABA triblock-graft copolymers based on PCL and PEG analogues. *Macromol. Res.* **2015**, *23*, 607−617.
31. Lutz, J.-F.; Weichenhan, K.; Akdemir, Ö.**;** Hoth, A. About the phase transitions in aqueous solutions of thermoresponsive copolymers and hydrogels based on 2-(2-methoxyethoxy)ethyl methacrylate and oligo(ethylene glycol) methacrylate. *Macromolecules* **2007**, *40*, 2503−2508.
32. Lin, W.C.; Liou, S.H.; Kotsuchibashi, Y. Development and characterisation of the imiquimod poly(2-(2-methoxyethoxy)ethyl methacrylate) hydrogel dressing for keloid therapy. *Polymers.* **2017**, *9*, 579.
33. Sun, S.T.; Wu, P.Y. On the thermally reversible dynamic hydration behavior of oligo(ethylene glycol) methacrylate-based polymers in water. *Macromolecules* **2013**, *46*, 236−246.
34. Xu, L.Q.; Yao, F.; Fu, G.D.; Kang, E.T. Interpenetrating network hydrogels via simultaneous "click chemistry" and atom transfer radical polymerization. *Biomacromolecules* **2010**, *11*, 1810–1817.
35. Lenoir, S.; Riva, R.; Lou, X.; Detrembleur, Ch.; Jérôme, R.; Lecomte, Ph. Ring-opening polymerization of α-

chloro-ε-caprolactone and chemical modification of poly (α-chloro-ε-caprolactone) by atom transfer radical processes. *Macromolecules* **2004**, *37*, 4055–4061.

36. Chen, J.C.; Liu, M.Z.; Gao, C.M.; Lü, S.Y.; Zhang, X.Y.; Liu, Z.; Self-assembly behavior of pH- and thermo-responsive hydrophilic ABCBA-type pentablock copolymers synthesized by consecutive RAFT polymerization. *RSC Adv.* **2013**, *3*, 15085–15093.
37. Mishra, A.K.; Vishwakarma, N.K.; Patel, V.K.; Biswas, C.S.; Paira, T.K.; Mandal, T.K.; Maiti, P.; Ray, B. Synthesis, characterization, and solution behavior of well-defined double hydrophilic linear amphiphilic poly (*N*-isopropylacrylamide)-*b*-poly (ε-caprolactone)-*b*-poly (*N*-isopropylacrylamide) triblock copolymers. *Colloid Polym. Sci.* **2014**, *292*, 1405–1418.
38. Ning, W.Y.; Shang, P.; Wu, J.; Shi, X.Y.; Liu, S.X. Novel amphiphilic, biodegradable, biocompatible, thermo-responsive ABA triblock copolymers based on PCL and PEG analogues via a combination of ROP and RAFT: synthesis, characterization, and sustained drug release from self-assembled micelles. *Polymers***. 2018**, *10*, 214.
39. Zhao,Y.P.; He, G.Q.; Guo, W.H.; Bao, L.L.; Yi, M.J.; Gong, Y.K.; Zhang, S.P. Self-assembled micelles prepared from amphiphilic copolymers bearing cell outer membrane phosphorylcholine zwitterions for a potential anti-phagocytic clearance carrier. *Polym. Chem.* **2016**, *7*, 5698–5708.
40. Li, S.S.; Chen, G.X.; Zhou, Z.; Li, Q.F. Stimuli-induced multiple dissociation and micellization transitions of random copolymers. *RSC Adv.* **2015**, *5*, 65847–65855.
41. Jin, N.X.; Zhang, H.; Jin, S.; Dadmun, M.D.; Zhao, B. Tuning of thermally induced sol-to-gel transitions of moderately concentrated aqueous solutions of doubly thermosensitive hydrophilic diblock copolymers poly(methoxytri(ethylene glycol) acrylate)-*b*-poly(ethoxydi(ethylene glycol) acrylate-*co*-acrylic acid). *J. Phys. Chem. B* **2012**, *116*, 3125–3137.